Results of the Department of Space Physics, Institute of Atmospheric Physics, Czech Academy of Sciences, published in 2018

1. Discovery of rapid whistlers close to Jupiter implying lightning rates similar to those on Earth

Electrical currents in atmospheric lightning strokes generate impulsive radio waves in a broad range of frequencies, called atmospherics. These waves can be modified by their passage through the plasma environment of a planet into the form of dispersed whistlers. In the Io plasma torus around Jupiter, Voyager 1 detected whistlers as several-seconds-long slowly falling tones at audible frequencies. These measurements were the first evidence of lightning at Jupiter. Subsequently, Jovian lightning was observed by optical cameras on board several spacecraft in the form of localized flashes of light. We analyzed measurements by the Waves instrument on board the Juno spacecraft that indicate observations of Jovian rapid whistlers: a form of dispersed atmospherics at extremely short timescales of several milliseconds to several tens of milliseconds. On the basis of these measurements, we reported over 1,600 lightning detections, the largest set obtained to date. The data were acquired during close approaches to Jupiter between August 2016 and September 2017, at radial distances below 5 Jovian radii. We detected up to four lightning strokes per second, similar to rates in thunderstorms on Earth and six times the peak rates from the Voyager 1 observations.

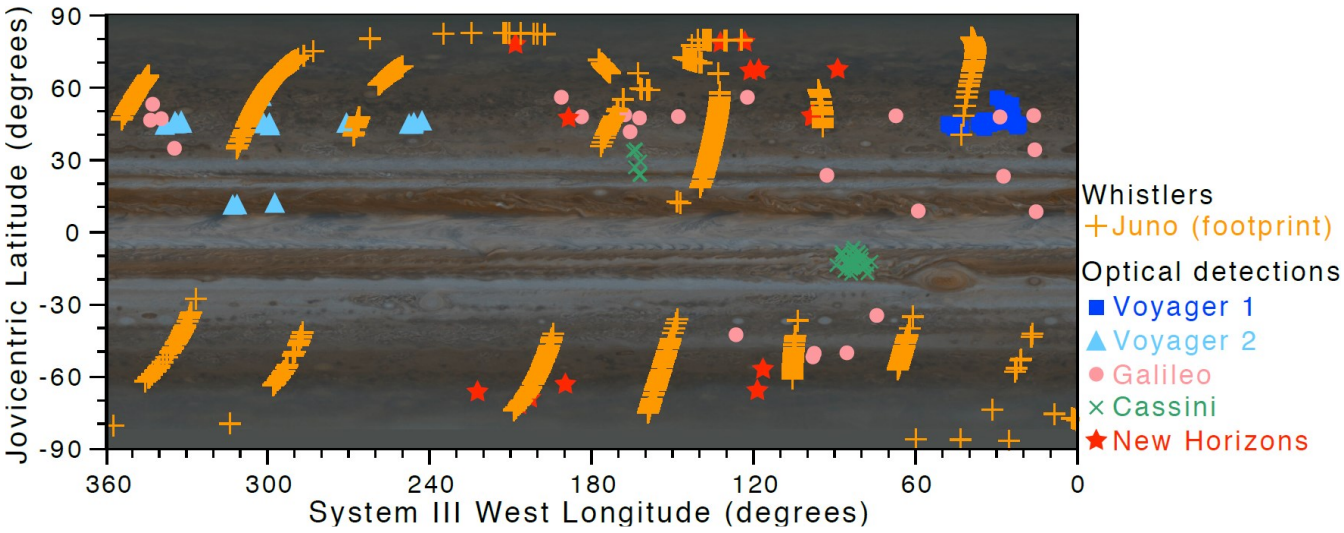

Map of lightning detections by the Juno Waves instrument compared with previous observations. projections along the model magnetic field lines from the Juno position down to an altitude of 300 km above the 1 bar level (which we assume is the bottom of the ionosphere) are plotted for 1,627 Jovian rapid whistlers by orange '+ ' signs, which also roughly indicate estimated uncertainties of lightning positions. Previous lightning observations are plotted for comparison: blue squares, Voyager 1 (36 lightning detections15); light blue triangles, Voyager 2 (18 detections4); pink dots, Galileo (estimated 336 flashes in 28 storms5,16); green crosses, Cassini (approximately 50 flashes in 4 spots6); red stars, New Horizons (18 flashes7). Electromagnetic detection by the Galileo probe17, and whistler observations by Voyager 1 (167 cases13) near the footprints of field lines passing through the high-density Io torus are not shown.

Reference:

Kolmašová, I., Imai, M., **Santolík, O.**, Kurth, W. S., Hospodarsky, G. B., Gurnett, D. A., Connerney, J. E. P., Bolton, S.J. (2018a), Discovery of rapid whistlers close to Jupiter implying lightning rates similar to those on Earth, Nature Astronomy, 2, 7, pp. 544-548.

Related references:

Brown, S., Janssen, M., Adumitroaie, V., Atreya, S., Bolton, S., Gulkis, S., Ingersoll, A., Levin, S., Li, Ch., Li, L., Lunine, J., Misra, S., Orton, G., Steffes, P., Tabataba-Vakili, F., **Kolmašová, I.,** Imai, M.**, Santolík, O.**, Kurth, W., Hospodarsky, G., Gurnett, D., Connerney, J. (2018), Prevalent lightning sferics at 600 megahertz near Jupiter's poles, Nature, 558, 87, pp. 87-90.

Imai, M., **Santolík, O.**, Brown, S. T., **Kolmašová, I.**, Kurth, W. S., Janssen, M. A., et al. (2018), Jupiter lightning-induced whistler and sferic events with waves and MWR during Juno perijoves. Geophysical Research Letters, 45, 7268-7276. https://doi.org/10.1029/2018GL078864.

Kurth, W. S., Mauk, B. H., Elliott, S. S., Gurnett, D. A., Hospodarsky, G. B., **Santolik, O.**, et al. (2018). Whistler mode waves associated with broadband auroral electron precipitation at Jupiter. Geophysical Research Letters, 45, 9372-9379. https://doi.org/10.1029/ 2018GL078566

2. Wave Polarization Analyzed by Singular Value Decomposition of the Spectral Matrix in the Presence of Noise

Analysis of wave polarization provides wave propagation parameters and enables an identification of modes in space plasmas, based on measurements of several components of fluctuating electromagnetic fields. This technique has become a conventional part of modern instrumentation onboard scientific spacecraft. A definition of the degree of polarization can be reduced to a very basic form, i.e., the ratio of a signal's polarized power to its total power. However, this simple definition can have several different realizations which depend mainly on the underlying assumptions about separating the polarized (coherent) part from the unpolarized part (noise). After reviewing polarization of a plane wave in two and three dimensions, we examined the singular value decomposition technique for a complex spectral matrix as well as for a real spectral matrix. We revisited the interpretation of singular values and we showed to what extent the singular values were able to contribute to a separation between polarized signal and noise. Finally, we verified our theoretical findings with synthetic data as well as with whistler-mode chorus wave observations from the THEMIS spacecraft.

Reference:

Taubenschuss, U. and Santolík, O. (2019), Wave Polarization analyzed by Singular Value Decomposition of the Spectral Matrix in the Presence of Noise, Surv. Geophys. 40, 39–69, https://doi.org/10.1007/s10712-018-9496-9 (Published on 19 August 2018).

Related references:

Němec, F., Hospodarsky, G. B., Bezdeková, B., Demekhov, A. G., Pasmanik, D., **Santolík, O.**, Kurth, W. S., and Hartley, D. (2018a), Quasiperiodic whistler mode emissions observed by the Van Allen Probes spacecraft. Journal of Geophysical Research: Space Physics, 123, 8969-8982. https://doi.org/10.1029/2018JA026058.

Němec, F., **Santolík, O.**, Boardsen, S. A., Hospodarsky, G. B., & Kurth, W. S. (2018b), Equatorial noise with quasiperiodic modulation: Multipoint observations by the Van Allen Probes spacecraft. Journal of Geophysical Research, 123, 4809-4819. https://doi.org/10.1029/2018JA025482.

Němec, F., **Santolík, O., Hayosh, M.**, Darrouzet, F., & Cornilleau-Wehrlin, N. (2018c), Detailed properties of equatorial noise with quasiperiodic modulation. Journal of Geophysical Research: Space Physics, 123, 5344-5355. https://doi.org/10.1029/2018JA025382.

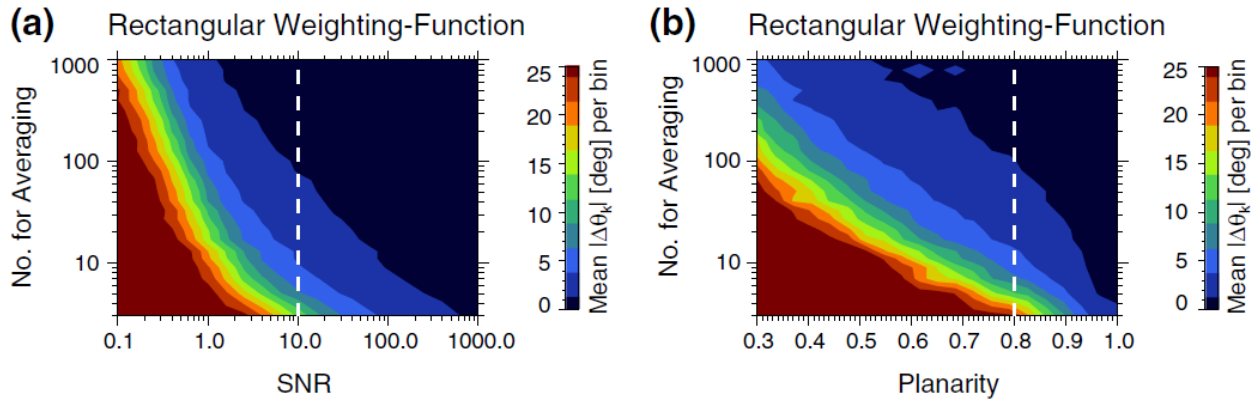

Absolute value of error in wave normal angle (Δk) as a function of a SNR and b planarity (x-axis) and the number of frequency channels over which spectral averaging is performed (y-axis).

3. Lightning initiation: Strong pulses of VHF radiation accompany preliminary breakdown

We analyzed lightning initiation process using magnetic field waveforms of preliminary breakdown (PB) pulses observed at time scales of a few tens of microseconds by a broad-band receiver. We compared these pulses with sources of narrow-band very high frequency (VHF) radiation at 60–66 MHz recorded by two separate Lightning Mapping Arrays (LMAs). We found that almost none of the observed PB pulses corresponded to geo-located VHF radiation sources, in agreement with previous results and with the hypothesis that processes generating VHF radiation and PB pulses are only weakly related. However, our detailed analysis discovered that individual peaks of strong VHF radiation seen by separate LMA

stations corresponded surprisingly well to the PB pulses. This result showed that electromagnetic radiation generated during fast stepwise extension of developing lightning channels was spread over a large interval of frequencies. We also showed that intense VHF radiation abruptly starts with the first PB pulse and that it was then continuously present during the entire PB phase of developing discharges.

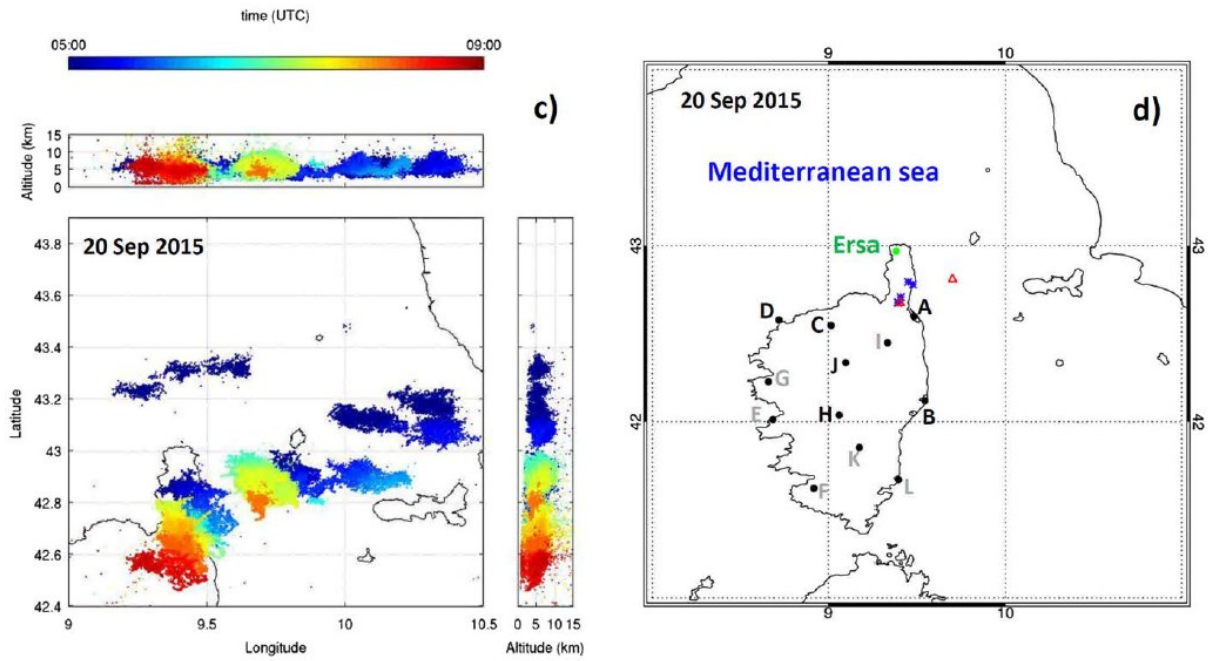

Maps: (left) VHF radiation sources geo-located by SAETTA on 20 September 2015. Color represents the time of observation of each source. (right) Configuration of instruments used in 2015. Green dots represent locations of broadband magnetic-field receivers, black dots show positions of LMA stations, blue stars and red triangles respectively represent negative cloud-to-ground and intracloud discharges identified by Météorage (no positive cloud-to-ground lightning was detected). The LMA stations used for our study are labeled by dark letters.

Reference:

Kolmašová, I., Santolik, O. Defer, E. Rison, W., Coquillat, S., Pedeboy, S., **Lán, R., Uhlíř, L**., Lambert, D. Pinty, J.-P. , Prieur, S. & Pont, V. (2018) Lightning initiation: Strong pulses of VHF radiation accompany preliminary breakdown. Scientific Reports 8, 3650, doi:10.1038/s41598-018-21972-z.

Related references:

Marshall, T., Bandara, S., Karunarathne, N., Karunarathne, S., **Kolmašová, I.**, Siedlecki, R., Stolzenburg, M. (2018): A study of lightning flash initiation prior to the first initial breakdown pulse, Atmospheric Research, 217, 1, pp. 10-23.

Bór, J., Zelkó, Z., Hegedüs, T., Jäger, Z., Mlynarczyk, J., **Popek, M.**, & Betz, H. D. (2018). On the series of +CG lightning strokes in dancing sprite events. Journal of Geophysical Research: Atmospheres, 123, 11,030–11,047. https://doi.org/10.1029/2017JD028251.

Špačková, H., Kolmašová, I., Santolík, O., Popek, M., and Bor, J. (2018), Properties of Sprite Parent Lightning for a Storm on 6 August 2013, in *WDS'18 Proceedings of Contributed Papers — Physics* (eds. J. Safrankova and J. Pavlu), Prague, Matfyzpress, pp. 93–98, 2018. ISBN 978-80-7378-374-7.

Záhlava, J., Nemec, F., **Santolík, O., Kolmašová, I.**, Parrot, M., & Kouba, D. (2018a). Selective attenuation of lightning-generated whistlers at extra low frequencies: DEMETER spacecraft observations. Journal of Geophysical Research: Space Physics, 123. https://doi.org/10.1029/2018JA025879.

Záhlava, J., Nemec, F., **Santolik, O., Kolmašova, I.**, Hospodarsky, G. B., Parrot, M., et al. (2018b). Longitudinal dependence of whistler mode electromagnetic waves in the Earth's inner magnetosphere. Journal of Geophysical Research: Space Physics, 123, 6562-6575. https://doi.org/10.1029/2018JA025284.

Záhlava, J., Nemec, F., Pincon, J. L., **Santolík, O., Kolmasová, I.**, & Parrot, M. (2018c). Whistler influence on the overall very low frequency wave intensity in the upper ionosphere. Journal of Geophysical Research: Space Physics, 123, 5648-5660. https://doi.org/10.1029/2017JA025137.

4. Interplanetary Type III Bursts and Electron Density Fluctuations in the Solar Wind

Type III bursts are generated by fast electron beams originated from magnetic reconnection sites of solar flares. As propagation of radio waves in the interplanetary medium is strongly affected by random electron density fluctuations, type III bursts provide us with a unique diagnostic tool for solar wind remote plasma measurements. We performed a statistical survey of 152 simple and isolated type III bursts observed by the twin-spacecraft Solar TErrestrial RElations Observatory mission. We investigated their time–frequency profiles in order to retrieve decay times as a function of frequency. Next, we performed Monte Carlo simulations to study the role of scattering due to random electron density fluctuations on time–frequency profiles of radio emissions generated in the interplanetary medium. For simplification, we assumed the presence of isotropic electron density fluctuations described by a power law with the Kolmogorov spectral index. Decay times obtained from observations and simulations were compared. We found that the characteristic exponential decay profile of type III bursts can be explained by the scattering of the fundamental component between the source and the observer despite restrictive assumptions included in the Monte Carlo simulation algorithm. Our results suggest that relative electron density fluctuations in the solar wind are 0.06–0.07 over wide range of heliospheric distances.

Reference:

Krupar, V., M. Maksimovic, E. P. Kontar, A. Zaslavsky, **O. Santolik, J. Soucek, O. Kruparova,** J. P. Eastwood, and A. Szabo (2018). Interplanetary Type III Bursts and Electron Density Fluctuations in the Solar Wind. Astrophysical Journal, 857:82 (7pp), 2018 April 20. https://doi.org/10.3847/1538-4357/aab60f.

Related references:

Grison, B., J. Soucek, V. Krupar, D. Písa, O.Santolík, U. Taubenschuss, and F. Nemec (2018). Shock deceleration in interplanetary coronal mass ejections (ICMEs) beyond Mercury's orbit until one AU. J. Space Weather Space Clim. 2018, 8, A54. https://doi.org/10.1051/swsc/2018043.

Erard, S., Cecconi, B., Le Sidaner, P., Rossi, A. P., Capria, M.T., Schmitt, B., Génot, V., André, N., Vandaele, A. C., Scherf, M., Hueso, R., Määttänen, A., Thuillot, W., Carry, B., Achilleos, N., Marmo, C., **Santolík, O.**, Benson, K., Fernique, P., Beigbeder, L., Millour, E., Rousseau, B., Andrieu, F., Chauvin, C., Minin, M., Ivanoski, S., Longobardo, A., Bollard, P., Albert, D., Gangloff, M., Jourdane, N., Bouchemit, M., Glorian, J. M., Trompet, L., Al-Ubaidi, T., Juaristi, J., Desmars, J., Guio, P., Delaa, O., Lagain, A**., Soucek, J., Píša, D.**.(2018), VESPA: A community-driven Virtual Observatory in Planetary Science, Planetary and Space Science, roc.150, pp. 65-85.

André, N., Grande, M., Achilleos, N., Barthélémy, M., Bouchemit, M., Benson, K., Blelly, P. L., Budnik, E., Caussarieu, S., Cecconi, B., Cook, T., Génot, V., Guio, P., Goutenoir, A., **Grison, B.**, Hueso, R., Indurain, M., Jones, G. H., Lilensten, J., Marchaudon, A., Matthiä, D., Opitz, A., Rouillard, A., Stanislawska, I., **Souček, J.**, Tao, C., Tomasik, L., Vaubaillon, J. (2018), Virtual Planetary Space Weather Services offered by the Europlanet H2020 Research Infrastructure, Planetary and Space Science, 150, pp. 50-59.

Bocchialini, K., **Grison, B.**, Menvielle, M., Chambodut, A., Cornilleau-Wehrlin, N., Fontaine, D., Marchaudon, A., Pick, M., Pitout, F., Schmieder, B., Régnier, S., Zouganelis, I., (2018), Statistical Analysis of Solar Events Associated with Storm Sudden Commencements over One Year of Solar Maximum During Cycle 23: Propagation from the Sun to the Earth and Effects, Solar Physics, 293, 5.

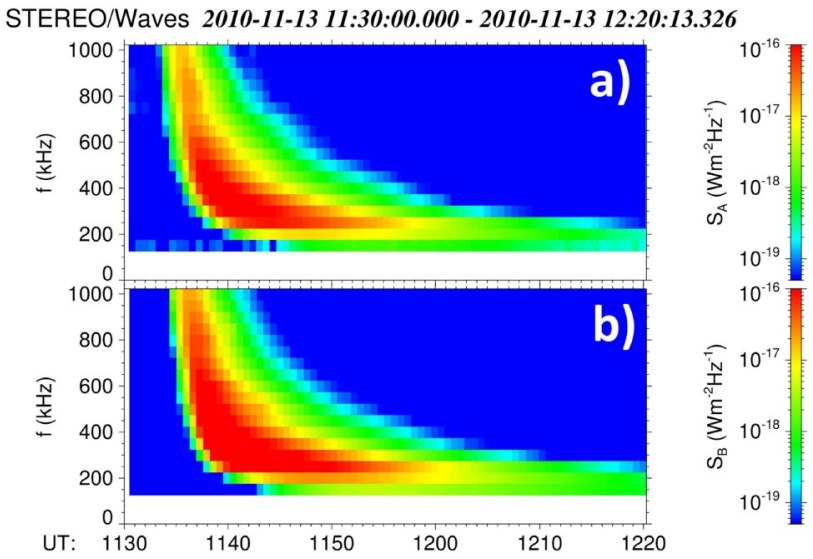

Radio measurements of the 2010 November 13 type III burst. (a), (b) Radio flux density S for STEREO-A and STEREO-B.

5. Plasmaspheric Plumes and EMIC Rising Tone Emissions

Due to its polar orbit Cluster spacecraft crossed plasmaspheric plumes out of the magnetic equatorial plane. We studied the occurrence of broadband, narrowband, and rising tone emissions in the plume vicinity, below the local proton gyrofrequency. Based on a database of 935 Cluster plumes crossings, reduced to 189 unique plumes, we found that broadband activity was the most common case. We confirmed result from a previous study showing that plume vicinity is not a preferred place for observing narrowband emissions. Rising tones are the less frequently observed of these three kinds of emissions. Nevertheless, ElectroMagnetic Ion Cyclotron (EMIC) rising tone occurrence rate was high compared to the narrowband one: Tones were seen in six of 30 plume events (20%) when narrowband emissions were observed. Rising tones were observed at absolute magnetic latitudes larger than 17° and up to 35°. Results of a ray tracing analysis agreed with a tone triggering process taking place above 15° of magnetic latitude.

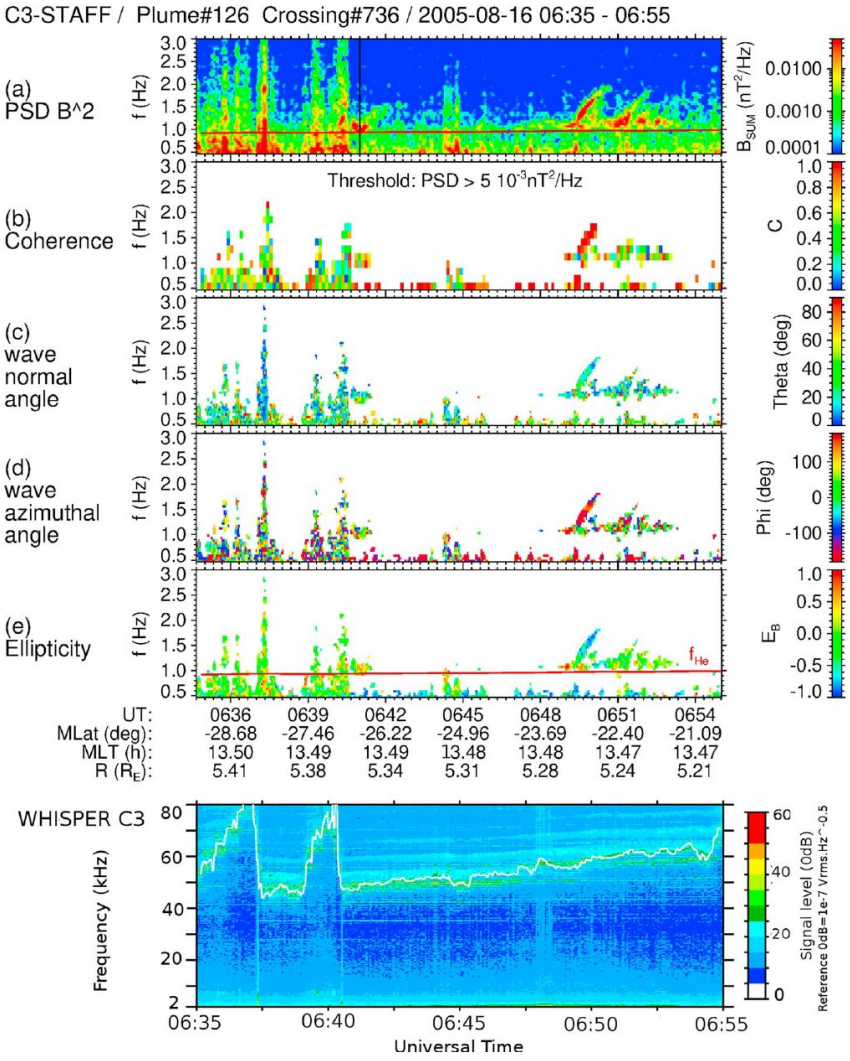

Wave and particle observations (16 August 2005). (top) wave properties (Cluster 3/STAFF-SC data): total magnetic power spectral density (a), coherence (b), wave normal angle (c), wave azimuthal angle (d), and ellipticity (e). Large rising tone is seen at 06:50 UT. Spacecraft exits the plume at 06:41 (vertical black

line, panel a). The 10-min lag between wave and particle windows takes into account Cluster 3/Cluster 4 separation. Bottom: time-frequency electric field spectrogram (Waves of High frequency and Sounder for Probing of Electron density by Relaxation (WHISPER) instrument). Plasma frequency is overplotted in white. STAFF-SC and WHISPER plots have the same timescale.

Reference:

Grison, B., Hanzelka, M., Breuillard, H., Darrouzet, F., **Santolík, O.**, Cornilleau-Wehrlin, N., & Dandouras, I. (2018b). Plasmaspheric plumes and EMIC rising tone emissions. Journal of Geophysical Research: Space Physics, 123, 9443-9452. https://doi.org/10.1029/2018JA025796.

Related references:

Hartley, D. P., Kletzing, C. A., **Santolík, O.,** Chen, L., & Horne, R. B. (2018). Statistical properties of plasmaspheric hiss from Van Allen Probes observations. Journal of Geophysical Research: Space Physics, 123, 2605-2619. https://doi.org/10.1002/2017JA02459.3

Tsurutani, B. T., Park, S. A., Falkowski, B. J., Lakhina, G. S., Pickett, J. S., Bortnik, J., Hospodarsky, G., **Santolik, O.,** Parrot, M., Henri, P., and Hajra, R. (2018). Plasmaspheric hiss: Coherent and intense. Journal of Geophysical Research: Space Physics, 123. https://doi.org/10.1029/2018JA025975.

Hartley, D. P., Kletzing, C. A., De Pascuale, S., Kurth, W. S., & **Santolík, O.** (2018), Determining plasmaspheric densities from observations of plasmaspheric hiss. Journal of Geophysical Research: Space Physics, 123, 6679-6691. https://doi.org/10.1029/2018JA025658.

6. Particle simulation of electromagnetic emissions from electrostatic instability driven by an electron ring beam on the density gradient

We analyzed the wave mode conversion between electrostatic and electromagnetic waves on the plasma density gradient. We used 2-D electromagnetic code KEMPO2 implemented with the generation of density gradient to simulate such a conversion process. In the dense region, we used ring beam instability to generate electron Bernstein waves and we studied the temporal evolution of wave spectra, velocity distributions, Poynting flux, and electric and magnetic energies to observe the wave mode conversion. Such a conversion process can be a source of electromagnetic emissions which are routinely measured by spacecraft on the plasmapause density gradient.

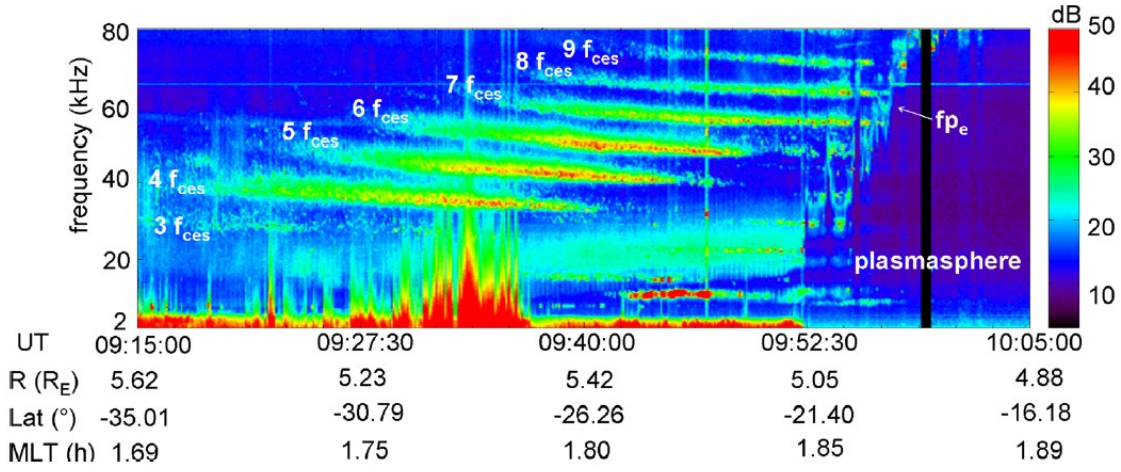

Frequency-time spectrogram of non-thermal continuum radiation close to the Earth's plasmapause observed by the WHISPER instrument onboard the Cluster 2 spacecraft on 15 February 2006. The wave intensity between 2 and 80 kHz is shown in dB above $10^{-8} mV^2_{rms} Hz^{-1}$. The spacecraft coordinates are given on the bottom: radial distance in Earth's radii, geomagnetic dipole latitude in degrees, and magnetic local time in hours.

Refrence:

Horký, M., Y. Omura, and **O. Santolík**, Particle simulation of electromagnetic emissions from electrostatic instability driven by an electron ring beam on the density gradient, Physics of Plasmas 25, 042905 (2018); https://doi.org/10.1063/1.5025912.

Related references:

Tichý, M., Petin, A., Kudrna, P., **Horký, M.**, Mazouffre, S., (2018), Electron energy distribution function in a low-power Hall thruster discharge and near-field plume, Physics of Plasmas, 25, 6.

7. First Observation of Lion Roar Emission in Saturn's Magnetosheath

We presented an observation of intense emissions in Saturn's magnetosheath as detected by the Cassini spacecraft. The emissions were observed in the dawn sector (magnetic local time ~06:45) of the magnetosheath over a time period of 11 h before the spacecraft crossed the bow shock and entered the unshocked solar wind. They were found to be narrow-banded with a peak frequency of about 0.16 f_{ce}, where f_{ce} is the local electron gyrofrequency. Using plane wave propagation analysis, we showed that the waves were right hand circularly polarized in the spacecraft frame and propagate at small wave normal angles (<10°) with respect to the ambient magnetic field. Electromagnetic waves with the same properties known as "lion roars" had been previously reported by numerous missions in the terrestrial magnetosheath. Here we showed the first evidence that such emissions exist outside the terrestrial environment. Our observations suggests that lion roars are a solar-system-wide phenomenon and

capable of existing in a broad range of parameter space. This also includes 1 order of magnitude difference in frequencies. Our result provided new insights into a new parameter regime characterized by a higher plasma beta (owing to the substantially higher Mach number bow shock) compared to Earth.

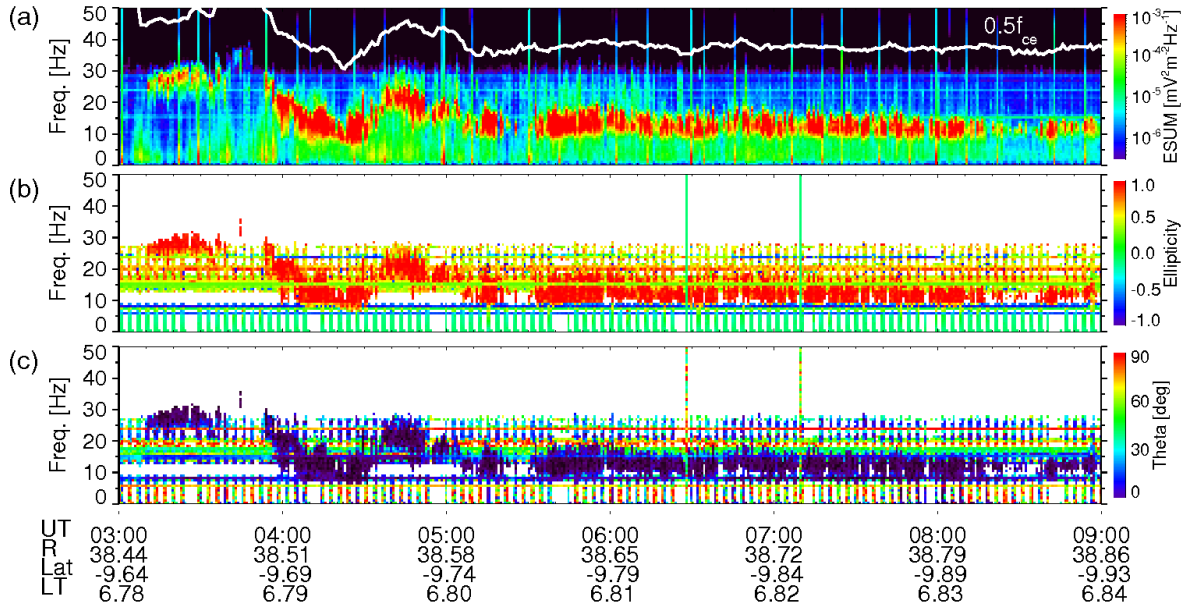

Cassini RPWS/WFR lower band data measured on 3 July 2005. (a and b) Sum of the power spectral densities of two components of electric field and three components of magnetic field, respectively, according to the color bars on the right-hand side, in the frequency range up to 50 Hz. The white line shows one half of the electron gyrofrequency, f_{ce}, calculated from 1 min fluxgate measurements. (c) Coherence in the polarization plane using the SVD method of the magnetic spectral matrices. (d) Ellipticity of the wave polarization combined with the sense of polarization, +1 for right-hand and -1 for the left-hand circularly polarized waves. (e) Polar angle of a wave vector, 0° for waves propagating parallel to the ambient magnetic field and 90° for transverse wave propagation. (f) Component of the Poynting flux along the ambient magnetic field with the level of confidence, positive values indicate parallel propagation and negative values antiparallel propagation.

Reference:

Píša, D., Sulaiman, A. H., **Santolík, O.**, Hospodarsky, G. B., Kurth, W. S., & Gurnett, D. A. (2018). First observation of lion roar emission in Saturn's magnetosheath. Geophysical Research Letters, 45. https://doi.org/10.1002/2017GL075919.

Related reference:

Sulaiman, A. H., Kurth, W. S., Hospodarsky, G. B., Averkamp, T. F., Persoon, A. M., Menietti, J. D., Ye, S. -Y., Gurnett, D. A., **Píša, D.,** Farrell, W.M., Dougherty, M. K., 2018: Auroral hiss emissions during Cassini, Geophysical Research Letters, 45, 14, pp. 6782-6789.

Department of Space Physics, Institute of Atmospheric Physics of the Czech Academy of Sciences in 2018

1. Radka Balková, secretary, 50% FTE, since November 1
2. Marek Basovník, PhD student, 60% FTE, until July 31
3. Benjamin Grison, research scientist
4. Michajlo Hajoš, research scientist
5. Miroslav Hanzelka, MSc student, 50% FTE until Sept 30, PhD student 70% FTE since October 1
6. Aaron T. Hendry, postdoctoral associate, since April 1
7. Miroslav Horký, postdoctoral associate
8. Petr Kašpar, postdoctoral associate
9. Andrea Kolínská, MSc student, 50% FTE, since June 1
10. Vratislav Krupař, research scientist, 50% FTE
11. Oksana Krupařová, research scientist, on maternal leave
12. Radek Lán, research engineer
13. Jan Lukačevič, research engineer until Sept 30, PhD student 70% FTE since October 1
14. Martin Pauer, research engineer, 20% FTE
15. David Píša, research scientist
16. Martin Popek, TLE observer, 25% FTE
17. Ondřej Santolík, senior research scientist, head of the department
18. Jan Souček, senior research scientist, deputy head of the department
19. Hana Špačková (née Zemanová), PhD student, 50% FTE until Sept 30, 70% FTE since October 1
20. Ulrich Taubenschuss, research scientist
21. Alexander Tomori, PhD student, 40% FTE
22. Christof Weber, postdoctoral associate